

# Path-Integral Renormalization Group Method for Numerical Study on Ground States of Strongly Correlated Electronic Systems

Tsuyoshi KASHIMA and Masatoshi IMADA

*Institute for Solid State Physics,  
University of Tokyo, 5-1-5 Kashiwanoha,  
Kashiwa, Chiba, 277-8581*

(Received October 26, 2018)

A new efficient numerical algorithm for interacting fermion systems is proposed and examined in detail. The ground state is expressed approximately by a linear combination of numerically chosen basis states in a truncated Hilbert space. Two procedures lead to a better approximation. The first is a numerical renormalization, which optimizes the chosen basis and projects onto the ground state within the fixed dimension,  $L$ , of the Hilbert space. The second is an increase of the dimension of the truncated Hilbert space, which enables the linear combination to converge to a better approximation. The extrapolation  $L \rightarrow \infty$  after the convergence removes the approximation error systematically. This algorithm does not suffer from the negative sign problem and can be applied to systems in any spatial dimension and arbitrary lattice structure. The efficiency is tested and the implementation explained for two-dimensional Hubbard models where Slater determinants are employed as chosen basis. Our results with less than 400 chosen basis indicate good accuracy within the errorbar of the best available results as those of the quantum Monte Carlo for energy and other physical quantities.

KEYWORDS: quantum simulation, strongly correlated electron systems, Hubbard model, numerical renormalization group

## §1. Introduction

In these decades, many numerical algorithms, such as exact diagonalizations, quantum Monte Carlo and density matrix renormalization group(DMRG), were proposed and were applied to many strongly correlated electron systems. Though the exact diagonalization method is the most straightforward one, the system size it can treat is smaller than that other methods can treat. Quantum Monte Carlo(QMC) method is a powerful technique for correlated electron systems and has been applied to various systems.<sup>1,2)</sup> In some systems such as fermion systems and frustrated spin systems, however, the QMC is known to suffer from the negative sign problem. Namely, the cancellation of positive and negative Monte Carlo samples occurs and makes it practically impossible to estimate physical values in the presence of statistical and round-off errors. DMRG<sup>3)</sup> is a very

powerful numerical renormalization method which does not suffer from any sign problem. However, because of the spatial renormalization process, DMRG is known to be applied efficiently only to one-dimensional configurations.

Path-integral renormalization group algorithm(PIRG) has been proposed<sup>7)</sup> as a new numerical algorithm for studying the ground state properties of strongly correlated fermion systems. The crucial point is that PIRG does not suffer from the negative sign problem and can be applied to any type of Hamiltonian in any dimension. The approximate ground state wavefunction is filtered out after numerical renormalization process in the path-integral formalism and expressed from the optimized linear combination of basis states in truncated Hilbert space. Since the explicit form of the wavefunction is obtained, the variational principle is satisfied and the method does not lead to the sign problem in contrast to QMC. Compared to DMRG, the numerical renormalization is done to the imaginary time direction irrespective of the spatial dimensionality of the system. Since the wavefunction is numerically given by using simple basis representation, it makes it easier to compute physical properties.

In Chapter 2, we will explain the whole ideas and procedures of PIRG, such as renormalization group method, truncated Hilbert subspace and extrapolation procedure, from the viewpoint of physical implications and compare PIRG with QMC and DMRG.

In Chapter 3, we will discuss the PIRG procedure from the viewpoint of implementation. There are some ideas and devices to make the PIRG calculation faster. We discuss the computation time and necessary computer memory. We review the structure of the PIRG procedure to discuss the parallelization of PIRG.

In Chapter 4, we test PIRG efficiency by applying this method to the two-dimensional Hubbard model with nearest-neighbor transfers and compare the results with those of exact diagonalization and QMC. We show that the PIRG gives the results with accuracy of around three digits for energy and around two digits for the momentum distributions and the spin correlations.

## §2. Path-Integral Renormalization Group Algorithm

### 2.1 The whole procedures of PIRG

PIRG method consists of the following procedures.

- Initial state.
  - It is possible to use any kind of initial state. Generally, closer to the ground state, better as an initial state and it is possible to use a linear combination of chosen basis states  $|\psi_{initial}\rangle = \sum_{i=1}^L c_i |\phi_i\rangle$  or to use a single basis state  $|\phi\rangle$ .
- Projection.
  - The projection operator is introduced by  $\exp(-\tau H)$  or by  $1 - \tau H$  to achieve the ground state. This projection expands the stored Hilbert subspace and thus the number of basis

states increases.

- Truncation.
  - Generally, the projection makes the number of basis states increase larger than our computer memory, or even if they can be stored, it is impossible to deal with them in the limited computer time. It is necessary to select important states and to keep the dimension of the stored Hilbert subspace  $L$ .
- Iteration.
  - By the projection process using proper projection operator and the truncation process, the numerical renormalization is achieved and the stored  $L$  dimensional subspace approaches the ground state. It is necessary to repeat this renormalization process until the lowest energy of the truncated Hilbert space converges to the lowest energy under the condition that the dimension of subspace is  $L$ .

Empirically, to achieve the best approximate ground state under the allowed dimension  $L$ , it is necessary to start PIRG using a good  $L = 1$  state. In fact, the best result at  $L = 1$  represents nothing but the optimized Hartree-Fock result. We start PIRG from  $L = 1$  and make  $L$  larger step by step, using the previous converged state as the initial state at next  $L$ -dimensional subspace. In addition to that, it is important for a faster convergence to iterate the renormalization process sufficiently at small  $L$ .

## 2.2 Renormalization group methods

### 2.2.1 Renormalization direction

The basic idea of the renormalization group methods is to keep the relevant information of a system and integrate out the irrelevant one. PIRG can be compared to the infinite-size system DMRG.<sup>3)</sup> In the infinite-size system DMRG, two single sites are inserted between the system-part and the environment-part to enlarge these two parts as shown in Fig.1. In this process, using the exactly represented single-site Hamiltonians, the stored states information increases temporarily before the truncation process and the relevant information of the ground state is stored. This process is allowed only for one-dimensional system because the dimension of the Hamiltonian matrix of two enlarged part, or the dimension of the temporarily expanded Hilbert subspace, is too large to treat for boundaries of multi-dimensional systems.

In contrast to DMRG, the numerical renormalization is performed in the imaginary time direction in PIRG. More concretely, the ground state  $|\psi_g\rangle$  is obtained by

$$|\psi_g\rangle = \lim_{\tau \rightarrow \infty} \exp[-\tau H]|\phi_0\rangle, \quad (2.1)$$

where  $|\phi_0\rangle$  is an initial state. Although the finite temperature DMRG<sup>4-6)</sup> has a similarity to this renormalization in the imaginary time direction, it can treat only the one-dimensional systems again

because the transfer matrix has to be utilized. Generally, the state  $|\psi_g\rangle$  can be represented as a linear combination of arbitrary basis states. However usually, the projection  $\lim_{\tau \rightarrow \infty} \exp[-\tau H]$  can not be performed in one operation. Following the Feynman's path-integral formalism, by taking sufficiently small  $\Delta\tau$ , the projection procedure may, for example, be given as,

$$|\psi_g\rangle = \lim_{\Delta\tau \rightarrow 0} \lim_{n \rightarrow \infty} (\exp[-\Delta\tau H])^n |\phi_0\rangle. \quad (2.2)$$

In quantum Monte Carlo methods, Eq.(2.2) is usually implemented at a fixed large  $n$  and sufficiently small  $\Delta\tau$  which are enough to filter out the ground state from the initial state  $|\phi_0\rangle$ . In the PIRG method, as in DMRG approach, two identical new projection operators  $\exp[-\Delta\tau \hat{H}]$  are inserted between the stored states  $|\psi_s\rangle$ . Namely, one operates to the right state  $|\psi_s\rangle$  while the other operates to the left state  $\langle\psi_s|$ . When the stored state  $|\psi_s\rangle$  is obtained after  $n$  projection steps from the initial state  $|\phi_0\rangle$ , the expectation value of a physical quantity  $\langle\hat{A}\rangle$  is represented by the initial state as

$$\frac{\langle\psi_s|\hat{A}|\psi_s\rangle}{\langle\psi_s|\psi_s\rangle} \Leftarrow \frac{\langle\phi_0|\exp[-\Delta\tau \hat{H}]^n \hat{A} \exp[-\Delta\tau \hat{H}]^n |\psi_0\rangle}{\langle\phi_0|\exp[-\Delta\tau \hat{H}]^n \exp[-\Delta\tau \hat{H}]^n |\psi_0\rangle}.$$

Here, ' $\Leftarrow$ ' indicates the truncation procedure in PIRG. After the step of the PIRG procedure, in other word, after the projection operators  $\exp[-\Delta\tau \hat{H}]$  are inserted, this expression is changed into the following form.

$$\begin{aligned} & \frac{\langle\psi_s|\exp[-\Delta\tau \hat{H}] \hat{A} \exp[-\Delta\tau \hat{H}] |\psi_s\rangle}{\langle\psi_s|\exp[-\Delta\tau \hat{H}] \exp[-\Delta\tau \hat{H}] |\psi_s\rangle} \\ \Leftarrow & \frac{\langle\phi_0|\exp[-\Delta\tau \hat{H}]^{n+1} \hat{A} \exp[-\Delta\tau \hat{H}]^{n+1} |\psi_0\rangle}{\langle\phi_0|\exp[-\Delta\tau \hat{H}]^{n+1} \exp[-\Delta\tau \hat{H}]^{n+1} |\psi_0\rangle}. \end{aligned}$$

Because the dimension of the Hilbert subspace increases in this projection process, the truncation process is necessary similarly to DMRG method. By this projection and truncation process, PIRG method achieves the numerical renormalization in the imaginary time direction which is represented in the path integral formalism.

### 2.2.2 Path integral formalism for the Hubbard model in the Slater determinant basis

The formalism given below shares the similarity to that of the auxiliary field Monte Carlo method.<sup>1)</sup> In this paper, we use the following Hubbard model Hamiltonian:

$$\begin{aligned} H &= H_k + H_U, \\ H_k &= - \sum_{\langle i,j \rangle, \sigma} t_{ij} \left( c_{i\sigma}^\dagger c_{j\sigma} + h.c. \right), \\ H_U &= U \sum_i \left( n_{i\uparrow} - \frac{1}{2} \right) \left( n_{i\downarrow} - \frac{1}{2} \right) \\ &= U \sum_i n_{i\uparrow} n_{i\downarrow} - U \left( M - \frac{N}{4} \right), \end{aligned} \quad (2.3)$$

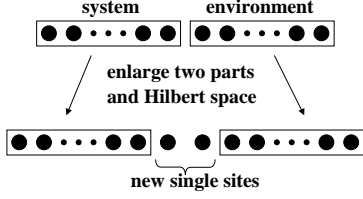


Fig. 1. Graphical representation of the one step of the infinite-size system DMRG. 1D-system is divided into two parts, the system and the environment. Each of them are enlarged by one site and in this process the Hilbert space is also enlarged by the exactly represented one-site Hamiltonian.

where  $i$  and  $j$  represent the lattice points,  $c_{i\sigma}^\dagger$  ( $c_{i\sigma}$ ) the creation (annihilation) operator of an electron with spin  $\sigma$  on the  $i$ -th site,  $n_{i\sigma} = c_{i\sigma}^\dagger c_{i\sigma}$ ,  $t_{ij}$  the transfer integral between the  $i$ -th site and the  $j$ -th site,  $U$  the on-site Coulomb interaction,  $M = \sum_{i,\sigma} n_{i\sigma}$  and  $N$  the number of the lattice sites.

The projecting operator can be divided into the kinetic and the interaction terms approximately.

$$\exp \left[ -\Delta\tau \left( \hat{H}_k + \hat{H}_U \right) \right] = \exp \left[ -\Delta\tau \hat{H}_k \right] \exp \left[ -\Delta\tau \hat{H}_U \right] + O \left( (\Delta\tau)^2 \right). \quad (2.4)$$

In this paper, we assume that the basis states are Slater determinants. Hereafter, we use the notation  $|\phi_\sigma\rangle$  to represent a Slater determinant with spin  $\sigma$  and  $|\phi\rangle = |\phi_\uparrow\rangle \otimes |\phi_\downarrow\rangle$ . Since a Slater determinant is a single particle state, the projection of single-body operator only changes a Slater determinant to other single Slater determinant. Namely,

$$\exp \left[ -\Delta\hat{H}_k \right] |\phi_\sigma\rangle = |\phi'_\sigma\rangle. \quad (2.5)$$

Though the interaction term is a many-body term, the projection term of it can be transformed into the sum of two single operator projections by using the Stratonovich variable  $s$ :

$$\begin{aligned} & \exp \left[ -\Delta\tau U n_{m\uparrow} n_{m\downarrow} \right] \\ &= \frac{1}{2} \sum_{s=\pm 1} \exp \left[ \alpha(s) n_{m\uparrow} \right] \exp \left[ \alpha(-s) n_{m\downarrow} \right], \end{aligned} \quad (2.6)$$

where

$$\alpha(s) = 2as - \frac{\Delta\tau U}{2}, \quad (2.7)$$

$$a = \tanh^{-1} \sqrt{\tanh \left( \frac{\Delta\tau U}{4} \right)}. \quad (2.8)$$

As a consequence,

$$\exp \left[ -\Delta\tau U n_{m\uparrow} n_{m\downarrow} \right] |\phi\rangle = \frac{1}{2} (|\phi^{m+}\rangle + |\phi^{m-}\rangle) \quad (2.9)$$

$$\exp[-\Delta\tau\hat{H}_U]|\phi\rangle = \sum_{i=1}^{2^N} |\phi_i\rangle \quad (2.10)$$

In this way, the projection of the local interaction term,  $\exp[-\Delta\tau U n_{m\uparrow} n_{m\downarrow}]$ , changes a Slater determinant to the sum of two Slater determinants. After the projection of the  $N$ -sites interaction term  $\exp[-\Delta\tau\hat{H}_U]$ , an original single Slater determinant expands to the sum over  $2^N$  Slater determinants. Though we use Slater determinants and a projection  $\exp[-\Delta\tau\hat{H}]$ , a similar dimensional expansion occurs even if we use other kind of basis states such as the site representation and a projection  $1 - \hat{H}$ . This is the reason why QMC sampling or PIRG truncation is necessary.

### 2.3 Truncated Hilbert space

#### 2.3.1 Variational principle

The expectation value  $\langle \rangle_g$  of a physical variable  $\hat{A}$  in the ground state  $|\psi_g\rangle$  can be calculated with an arbitrary complete set of basis states  $|\phi_i\rangle$  as follows:

$$\begin{aligned} |\psi_g\rangle &= \sum_i^{D_{Hilbert}} |\phi_i\rangle, \\ \langle \hat{A} \rangle_g &= \frac{\sum_{i,j}^{D_{Hilbert}} \langle \phi_i | \hat{A} | \phi_j \rangle}{\sum_{i,j}^{D_{Hilbert}} \langle \phi_i | \phi_j \rangle}. \end{aligned} \quad (2.11)$$

However, the sum in the above equation is practically impossible in general for easily available basis states because the number of them,  $D_{Hilbert}$ , is usually comparable to the dimension of the whole Hilbert space. QMC methods deal with this problem by sampling the numerator and the denominator separately:

$$\langle \hat{A} \rangle \approx \frac{\sum_{(a,b)}^{N_s} \left( \overbrace{\frac{\|\langle \phi_a | \phi_b \rangle\|}{\sum_{i,j}^{D_{Hilbert}} \|\langle \phi_i | \phi_j \rangle\|}}^{\text{Probability}} \times \overbrace{\frac{\langle \phi_a | \phi_b \rangle}{\|\langle \phi_a | \phi_b \rangle\|}}^{\text{Sign}} \times \overbrace{\frac{\langle \phi_a | \hat{A} | \phi_b \rangle}{\langle \phi_a | \phi_b \rangle}}^{\text{Sample}} \right)}{\sum_{(c,d)}^{N_s} \left( \underbrace{\frac{\|\langle \phi_c | \phi_d \rangle\|}{\sum_{i,j}^{D_{Hilbert}} \|\langle \phi_i | \phi_j \rangle\|}}_{\text{Probability}} \times \underbrace{\frac{\langle \phi_c | \phi_d \rangle}{\|\langle \phi_c | \phi_d \rangle\|}}_{\text{Sign}} \right)} \quad (2.12)$$

where  $\|\|\|$  represents the absolute value and  $N_s$ , the number of Monte Carlo samples. Usually, these sampling processes are taken for an identical set  $(c, d) = (a, b)$  in the Metropolis algorithm.

Because the diagonal elements  $\langle \phi_a | \phi_a \rangle$  are not necessarily contained in Monte Carlo samples and  $\langle \phi_a | \phi_b \rangle$  in the sum are taken only partially by sampling, QMC does not satisfy the variational principle in the strict sense, although the deviation should be within the range of statistical error. Several thousands samples are practically taken, to reach the accuracy with a relative error less than a few percents. In case of the system with the sign problem, however, it is difficult to achieve the same accuracy by this sampling process.

On the contrary, the variational principle is satisfied and the sign problem is absent in PIRG because the ground state is represented approximately as a linear combination of arbitrary basis states.

$$|\psi_g\rangle \approx |\psi\rangle = \sum_{i=1}^L w_i |\phi_i\rangle. \quad (2.13)$$

In Eq.(2.13),  $|\phi_i\rangle$  are optimal basis states in the whole Hilbert space. For example, orthogonal basis states such as site-represented ones or non-orthogonal basis states such as Slater determinants can be used. In any case, to take the sum in Eq.(2.11) within the allowed computation time, these basis states should be simple ones and the number of them,  $L$ , be small. Of course, the relation between  $L$  and the truncation error may depend on the choice of basis states. Although we discuss the relation next, we do not know it clearly now. Empirically, as we show the results in Chapter 4, with the choice of the Slater determinant bases, limited and tractable basis states, such as hundreds basis states, can reach the ground state with the relative error less than a few percents for most of physical quantities of our interest even when the Hilbert space is enormously large.

From theoretical and practical viewpoints, the relation between the error of estimated properties and the truncated Hilbert space dimensions  $L$  is very important. It is known that the relative error decreases exponentially in DMRG<sup>3)</sup> when the number of states kept, or the dimension of the subspace, increases. This makes DMRG powerful. In DMRG, because the states are not treated explicitly, there is no restriction on the choice of bases. Namely, although both PIRG and DMRG are the methods to make the truncated Hilbert space converge to the ground state, the restrictions posed on the choice of basis states are different in two methods.

### 2.3.2 The lowest energy in the truncated Hilbert space

As shown in Eq.(2.13), the stored approximate ground state is represented as,

$$|\psi\rangle = \sum_{i=1}^L w_i |\phi_i\rangle$$

Because the basis states  $|\phi_i\rangle$  which constitute the stored Hilbert subspace are chosen so as to give the lowest energy within the allowed dimensions of the Hilbert subspace, it is necessary to optimize the coefficient  $w_i$  in every truncation process. The energy  $E$  of the state  $|\psi\rangle$  follows the equation,

$$E = \frac{\sum_{i,j=1}^L [H]_{ij} w_i w_j}{\sum_{i,j=1}^L [F]_{ij} w_i w_j} \quad (2.14)$$

where,

$$\begin{aligned} [H]_{ij} &= \langle \phi_i | \hat{H} | \phi_j \rangle \\ [F]_{ij} &= \langle \phi_i | \phi_j \rangle. \end{aligned} \quad (2.15)$$

The lowest energy  $E$  in this subspace is the lowest eigenvalue of this subspace. Then, to obtain

the lowest energy and its state, we solve the following generalized eigenvalue problem.

$$\sum_{j=1}^L [H]_{ij} w_i = E \sum_{j=1}^L [F]_{ij} w_j. \quad (2.16)$$

#### 2.4 Extrapolation on the dimension of the stored subspace to the dimension of the whole Hilbert space

##### 2.4.1 Extrapolation of energy

We need the extrapolation procedure to large  $L$  to estimate the systematic deviation, because the exact value is achieved only when  $L$  becomes the dimension of the whole Hilbert space. In practice it is difficult to analyze the relation between the dimension  $L$  and the systematic deviation of expectation values. In addition to that, the relation may depend on the choice of the bases. Therefore, we do not use the argument  $L$  in the extrapolation function and introduce another extrapolation procedure. The important point is that the extrapolation procedure gives more accurate estimate. We, however, note that after this extrapolation, the variational principle may not necessarily be satisfied because the obtained energy could be lower than the exact one within the extrapolation error. We define the difference between the ground state energy and the expectation value in a given subspace as

$$\delta E = \langle \hat{H} \rangle - \langle \hat{H} \rangle_g \quad (2.17)$$

It can be shown<sup>8)</sup> that the difference  $\delta E$  vanishes linearly as a function of the energy variance  $\Delta E$  defined by

$$\Delta E = \frac{\langle \hat{H}^2 \rangle - \langle \hat{H} \rangle^2}{\langle \hat{H} \rangle^2} \quad (2.18)$$

We summarize the proof of this in the following way: First we put the approximate ground state  $|\psi\rangle$  as

$$\begin{aligned} |\psi\rangle &= c|\psi_g\rangle + d|\psi_e\rangle \\ c^2 + d^2 &= 1 \end{aligned} \quad (2.19)$$

where  $|\psi_g\rangle$  and  $|\psi_e\rangle$  are orthonormalized states. We also define

$$\begin{aligned} D_1 &\equiv \frac{\langle \hat{H} \rangle_e - \langle \hat{H} \rangle_g}{\langle \hat{H} \rangle_g}, \\ D_2 &\equiv \frac{\langle \hat{H}^2 \rangle_e - \langle \hat{H} \rangle_g^2}{\langle \hat{H} \rangle_g^2}, \\ D_3 &\equiv \frac{\langle \hat{H}^3 \rangle_e - \langle \hat{H} \rangle_g^3}{\langle \hat{H} \rangle_g^3}, \end{aligned} \quad (2.20)$$

where

$$\langle \hat{A} \rangle_g = \frac{\langle \psi_g | \hat{A} | \psi_g \rangle}{\langle \psi_g | \psi_g \rangle}, \quad \langle \hat{A} \rangle_e = \frac{\langle \psi_e | \hat{A} | \psi_e \rangle}{\langle \psi_e | \psi_e \rangle}. \quad (2.21)$$

In this notation,

$$\begin{aligned}
\langle \hat{H} \rangle &= \langle \hat{H} \rangle_g + d^2 \langle \hat{H} \rangle_g D_1 \\
\langle \hat{H}^2 \rangle &= \langle \hat{H} \rangle_g^2 + d^2 \langle \hat{H} \rangle_g^2 D_2 \\
\langle \hat{H}^3 \rangle &= \langle \hat{H} \rangle_g^3 + d^2 \langle \hat{H} \rangle_g^3 D_3 \\
\Rightarrow &\begin{cases} \delta E = d^2 E_0 D_1 \\ \Delta E = d^2 (D_2 - 2D_1) + d^4 D_1 (3D_1 - 2D_2) + O(d^6) \end{cases} .
\end{aligned} \tag{2.22}$$

where  $\langle \hat{A} \rangle = \langle \psi | \hat{A} | \psi \rangle / \langle \psi | \psi \rangle$  and  $E_0 \equiv \langle \hat{H} \rangle_g$ . When the stored state  $|\psi\rangle$  is a good approximation of the ground state, the coefficient  $d$  is expected to be small. Then up to  $O(d^3)$ ,

$$\delta E \propto \Delta E \tag{2.23}$$

is satisfied. This is the simplest extrapolation procedure we introduce.

We may introduce other series of extrapolation procedure. They are more time consuming but can be more accurate. As we discussed in the renormalization procedure, there are operators that can make a state closer to the ground state. Here we take this kind of projection operator  $\hat{R}$ . In this case, for more accurate extrapolation,  $\delta E$  and  $\Delta E$  in the above simplest extrapolation procedure should be calculated on the state  $\hat{R}|\psi\rangle$ . Namely, in the above equations for any operators  $\hat{A}$ ,

$$\langle \hat{A} \rangle = \frac{\langle \psi | \hat{R}^\dagger \hat{A} \hat{R} | \psi \rangle}{\langle \psi | \hat{R}^\dagger \hat{R} | \psi \rangle} \tag{2.24}$$

may give a better estimate than that from  $\langle \psi | \hat{A} | \psi \rangle / \langle \psi | \psi \rangle$ . In the renormalization procedure, we have to consider the restriction of the Hilbert subspace dimension due to computer power. As shown in the above, however, if it is possible to calculate in the form Eq.(2.24) with the projection  $\hat{R}$ , it is equivalent to calculate the physical value with the state  $\hat{R}|\psi\rangle$ , which is in a larger Hilbert subspace than that the state  $|\psi\rangle$  belongs.

As an example of the projection operator  $\hat{R}$ , we take a function of Hamiltonian  $\hat{H}$ . When the absolute value of the ground state energy is the largest in all the eigenvalues, operating the Hamiltonian  $\hat{H}$  makes a state closer to the ground state. From a viewpoint of computation time, the number of the terms contained in the Hamiltonian of the system without any long-range interaction is the order of  $N$ . If we take the Hamiltonian  $\hat{H}$  as the projection operator  $\hat{R}$ , it is necessary to calculate  $\langle \hat{H}^4 \rangle$  in  $\Delta E$  but it is not practical because the computation time increases to the order of  $N^4$ . Therefore in this paper we take  $\sqrt{\hat{H}}$  as the projection operator. To obtain the expectation value of  $\hat{A}$  on the state  $\hat{R}|\phi\rangle$ , we use Eq.(2.24). In this case, Eq.(2.22) is modified to the following.

$$\delta E \rightarrow \delta E_{sqr} = \frac{\langle \hat{H}^2 \rangle}{\langle \hat{H} \rangle} - \langle \hat{H} \rangle_g. \tag{2.25}$$

$$\Delta E \rightarrow \Delta E_{sqr} = \frac{\langle \hat{H}^3 \rangle \langle \hat{H} \rangle - \langle \hat{H}^2 \rangle^2}{\langle \hat{H}^2 \rangle^2}. \quad (2.26)$$

The difference  $\delta E_{sqr}$  is always smaller than the difference  $\delta E$  and the extrapolation procedure can be done closer to the ground state if we use  $\delta E_{sqr}$  and  $\Delta E_{sqr}$ . One might consider a problem whether the operator  $\sqrt{\hat{H}}$  exists or not. In the representation of  $\delta E_{sqr}$  and  $\Delta E_{sqr}$ , however,  $\sqrt{\hat{H}}$  does not appear but only  $\hat{H}$  does and the argument for  $\delta E_{sqr}$  and  $\Delta E_{sqr}$  remains correct. Even if we ignore the projection operator  $\hat{R} = \sqrt{\hat{H}}$  in Eq.(2.24) and only use Eq.(2.26), the following equations are obtained.

$$\Rightarrow \begin{cases} \delta E_{sqr} = d^2 E_0 (D_2 - D_1) \\ \quad + d^4 E_0 D_1 (2D_1 - D_2) + O(d^6) \\ \Delta E_{sqr} = d^2 (D_3 + D_1 - 2D_2) \\ \quad + d^4 (D_3 D_1 - 2D_2 D_3 - 2D_1 D_2 + 3D_2^2) + O(d^6) \end{cases} \quad (2.27)$$

By the same reason as that of the simple extrapolation procedure, the above equation leads to

$$\delta E_{sqr} \propto \Delta E_{sqr}. \quad (2.28)$$

Because both extrapolations are on the energy difference and the energy variance, they can be plotted on the same parameter plane. As shown in the above, however, two extrapolation plots are on different lines.

$$\delta E \approx \frac{D E_0}{D_2 - 2D} \Delta E \quad (2.29)$$

$$\delta E_{sqr} \approx \frac{(D_2 - D) E_0}{D_3 + D - 2D_2} \Delta E, \quad (2.30)$$

where the proportionality coefficients are different between Eq.(2.29) and Eq.(2.30). In this paper we use the  $\delta E_{sqr} - \Delta E_{sqr}$  extrapolation to examine the accuracy of the ground state energy.

#### 2.4.2 Extrapolation of other physical values

Because no commutation relation is expected between most operators of the physical quantity  $\hat{A}$  and Hamiltonian  $\hat{H}$ ,

$$\frac{\langle \phi | \sqrt{\hat{H}} \hat{A} \sqrt{\hat{H}} | \phi \rangle}{\langle \phi | \sqrt{\hat{H}} \sqrt{\hat{H}} | \phi \rangle} \neq \frac{\langle \phi | \hat{H} \hat{A} | \phi \rangle}{\langle \phi | \hat{H} | \phi \rangle}.$$

Then we can not use the above second extrapolation procedure. From the same reason as the computation time for obtaining the energy, higher order projection is not practically possible within our accessible computer power. For the moment, we do not know the suitable projection operator  $\hat{R}$ . Then, we use the simple extrapolation for other physical values than the energy. Some modifications are, however, necessary in the above discussion. The expectation value of  $\hat{A}$  is

$$\begin{aligned} \langle \hat{A} \rangle &= \langle \hat{A} \rangle_g + d^2 \langle \hat{A} \rangle_g D_A + 2cd \langle \psi_e | \hat{A} | \psi_g \rangle, \\ D_A &\equiv \frac{\langle \hat{A} \rangle - \langle \hat{A} \rangle_g}{\langle \hat{A} \rangle_g}. \end{aligned} \quad (2.31)$$

Different from the discussion on the extrapolation of the energy, in which the energy difference and the energy variance is proportional to  $d^2$ , the third term in  $\langle \hat{A} \rangle$  is proportional to  $d$  and therefore, the extrapolation of the expectation value of the operator  $\hat{A}$  should be done on the square root of the energy variance. Empirically, however, the  $d$  term is so small that it is easy to do the extrapolation on  $\langle \hat{A} \rangle$  linearly to the energy variance  $\Delta E$ , and we do so in this paper. Theoretically, it has been proven<sup>8)</sup> that if the operator  $\hat{A}$  is a short-ranged correlation function,  $\langle \psi_e | \hat{A} | \psi_g \rangle$  in Eq.(2.31) becomes zero in the thermodynamic limit as the following: Because  $|\psi_g\rangle$  and  $|\psi_e\rangle$  are orthonormalized states,

$$\begin{aligned} \left| \langle \psi_g | \hat{A} | \psi_e \rangle \right|^2 &= \left| \langle \psi_g | \hat{A} - \langle \hat{A} \rangle_g | \psi_e \rangle \right|^2 \\ &\leq \left\langle \left( \hat{A} - \langle \hat{A} \rangle_g \right)^2 \right\rangle_g \end{aligned} \quad (2.32)$$

where the latter inequality is led by Schwartz inequality and  $\langle \cdot \rangle_g = \langle \psi_g | \cdot | \psi_g \rangle$ . When  $\hat{A}$  is a short-ranged correlation function, the final term is proportional to  $1/N$  and becomes zero in the thermodynamic limit.

These extrapolation procedures on energy and other physical values are satisfied in a general ground state. They are not necessarily restricted to the purpose of the application in PIRG method and not necessarily for studying the ground state. It is possible to generalize these extrapolation procedures for obtaining a more accurate eigenstate properties from a series of approximations of eigenstate.

### 2.4.3 Comparison with previous methods

Truncations of the Hilbert space were used in many numerical method. Although DMRG is one of the most remarkable approaches, many other algorithms applicable to higher-dimensional systems have also been proposed.

Exact diagonalization method combined with the truncation of the Hilbert space<sup>9-11)</sup> can treat larger systems than a normal exact diagonalization method can do. The efficiency of the usage of basis state, however, is not sufficient partly because the basis states are in site-representation. Therefore the convergence of the energy as a function of the dimension of Hilbert subspace is much worse than that of PIRG which uses Slater determinants for basis states.

On the other hand, the quantum Monte Carlo method is also combined with the truncation of the Hilbert space and applied to fermion systems<sup>12)</sup> and boson systems.<sup>13)</sup> Although in these methods, candidate basis states are generated by Monte Carlo process of the whole Hamiltonian, in our experience, it is crucial for the lowering of the energy to make the acceptance of them higher by sequentially generating local, or one-site, projection. Renormalization and projection through the interaction term is achieved more efficiently by the local algorithms as we discuss in § 3.2.1. Several devices to get out of local minima and to realize global minimum are important in models of condensed matter systems.

A large difference between the above numerical algorithm and PIRG is the presence of the combined extrapolation procedure. It can make errors smaller systematically.

### §3. On the implementation of PIRG

#### 3.1 Matrix representation

The basic ideas of the following discussion are published.<sup>1)</sup> At first, we explain the expression of states and expectation values. A Slater determinant  $|\phi_\sigma\rangle$  is represented as an  $N \times M$  matrix  $[\phi_\sigma]$ .

$$|\phi_\sigma\rangle = \prod_{j=1}^M \left( \sum_{i=1}^N [\phi_\sigma]_{ij} c_{i\sigma}^\dagger \right) |0\rangle \quad (3.1)$$

The inner product of two Slater determinants is

$$\langle \phi_{a\sigma} | \phi_{b\sigma} \rangle = \det \left( {}^t [\phi_{a\sigma}] [\phi_{b\sigma}] \right). \quad (3.2)$$

(See Appendix). The matrix elements for the Hamiltonian and other operators are calculated from single-particle Green's function using the Wick's theorem, because a Slater determinant is a single-particle state. A single-particle Green's function  $[G_\sigma]$ , which is represented as an  $N \times N$  matrix, is calculated by

$$\begin{aligned} [G_\sigma^{ab}]_{ij} &= \frac{\langle \phi_{a\sigma} | c_{i\sigma}^\dagger c_{j\sigma} | \phi_{b\sigma} \rangle}{\langle \phi_{a\sigma} | \phi_{b\sigma} \rangle} \\ &= \sum_{k=1}^M \sum_{l=1}^M [\phi_{b\sigma}]_{ik} [g_\sigma^{ab}]_{kl} [\phi_{a\sigma}]_{jl} \end{aligned} \quad (3.3)$$

where

$$[g_\sigma^{ab}] = \left( {}^t [\phi_{a\sigma}] [\phi_{b\sigma}] \right)^{-1}. \quad (3.4)$$

The procedure to use the Wick's theorem is explained in the literature.<sup>1)</sup> Since the stored state in PIRG is a linear combination of Slater determinants, the expectation value of physical variables can be calculated from one-particle Green's functions between all the stored Slater determinants by using the Wick's theorem.

Next we explain the projection processes following the above representation. The kinetic term projection, Eq.(2.5), is expressed by using an  $N \times N$  matrices  $[M_0]$  and  $[K]$  in the following way:

$$[\phi'_\sigma]_{ij} = \sum_{k=1}^N [M_0]_{ik} [\phi_\sigma]_{kj} \quad \text{for } \sigma = \uparrow, \downarrow \quad (3.5)$$

where

$$\begin{aligned} [M_0] &= \exp[K] \\ [K]_{ij} &= -\Delta\tau t_{ij}. \end{aligned} \quad (3.6)$$

From Eq.(2.6) the local-interaction term projection, Eq.(2.9), is expressed as the following:

$$\begin{aligned} |\phi^{m+}\rangle &= \left( \sum_{k=1}^N [M_1(1)]_{ik} [\phi_{\uparrow}]_{kj} \right) \otimes \left( \sum_{k=1}^N [M_1(-1)]_{ik} [\phi_{\downarrow}]_{kj} \right) \\ |\phi^{m-}\rangle &= \left( \sum_{k=1}^N [M_1(-1)]_{ik} [\phi_{\uparrow}^{m-1}]_{kj} \right) \otimes \left( \sum_{k=1}^N [M_1(1)]_{ik} [\phi_{\downarrow}]_{kj} \right), \end{aligned} \quad (3.7)$$

where  $M_1$  is an  $N \times N$  matrix,

$$[M_1(s)]_{ij} = \begin{cases} \exp\left[2as - \frac{\Delta\tau U}{2}\right] & \text{for } i = j = m \\ 1 & \text{for } i = j, \quad i \neq m \\ 0 & \text{otherwise} \end{cases}. \quad (3.8)$$

## 3.2 Computation time

### 3.2.1 Whole procedures of the renormalization group method

Empirically we find that it is better to perform the projection and truncation at the projection of every local-interaction term  $\exp[-\Delta\tau U n_{m\uparrow} n_{m\downarrow}]$ . Hence we employ this *local algorithm*. Using this local algorithm, we summarize below how one PIRG iteration step  $\exp[-\Delta\tau \hat{H}] \left[ \sum_{a=1}^L c_a |\phi_a\rangle \right]$  proceeds. Note that in this paper  $|\phi_a\rangle$  represents  $|\phi_{a\uparrow}\rangle \otimes |\phi_{a\downarrow}\rangle$ , namely a direct product of Slater determinants for each spin.

- Choose one basis state.
  - Choose  $|\phi_a\rangle$  from  $L$  stored basis states  $\{|\phi_1\rangle, |\phi_2\rangle, \dots, |\phi_L\rangle\}$ , which will be operated by  $\exp[-\Delta\tau \hat{H}]$
- Projection by  $\exp[-\Delta\tau \hat{H}_k]$ .
  - $\Rightarrow$  *computation time*  $\propto (LN^3 + L^3)$
  - Perform  $|\phi'_a\rangle = \exp[-\Delta\tau \hat{H}_k] |\phi_a\rangle$  following Eq.(2.5) and calculate the inner products and Hamiltonian elements between

$$|\phi'_a\rangle$$

and

$$\{|\phi_1\rangle, |\phi_2\rangle, \dots, |\phi_{a-1}\rangle, |\phi_{a+1}\rangle, \dots, |\phi_L\rangle\}.$$

$\rightarrow$  *computation time*  $\propto LN^3$

- Truncation is performed by comparing the lowest energies obtained from Eq.(2.16) in two subspaces which consist of the following two sets of  $L$  basis states:

$$\begin{cases} \{|\phi_1\rangle, |\phi_2\rangle, \dots, |\phi_{a-1}\rangle, |\phi_a\rangle, |\phi_{a+1}\rangle, \dots, |\phi_L\rangle\} \\ \{|\phi_1\rangle, |\phi_2\rangle, \dots, |\phi_{a-1}\rangle, |\phi'_a\rangle, |\phi_{a+1}\rangle, \dots, |\phi_L\rangle\} \end{cases}$$

and by employing one of these two basis states set which gives the lower energy. In other words, take  $|\phi_a\rangle$  or  $|\phi'_a\rangle$  to be a next basis state  $|\phi_a^0\rangle$ .

$\rightarrow$  *computation time*  $\propto L^3$

- Projection by  $\exp[-\Delta\tau\hat{H}_U]$ .  
 $\Rightarrow$  *computation time*  $\propto (LN^3 + L^3N)$
- Perform

$$\frac{1}{2}(|\phi_a^{m+}\rangle + |\phi_a^{m-}\rangle) = \exp[-\Delta\tau U n_{m\uparrow} n_{m\downarrow}] |\phi_a^{m-1}\rangle$$

following Eq.(2.9) and calculate the inner products and Hamiltonian elements between

$$|\phi_a^{m+}\rangle \quad \text{or} \quad |\phi_a^{m-}\rangle$$

and

$$\{|\phi_1\rangle, |\phi_2\rangle, \dots, |\phi_{a-1}\rangle, |\phi_{a+1}\rangle, \dots, |\phi_L\rangle\}.$$

$\rightarrow$  *computation time*  $\propto LN^2$

- Truncation is performed by comparing the lowest energies obtained from Eq.(2.16) in three subspaces which consist of the following three sets of  $L$  basis states:

$$\begin{cases} \{|\phi_1\rangle, |\phi_2\rangle, \dots, |\phi_{a-1}\rangle, |\phi_a^{m-1}\rangle, |\phi_{a+1}\rangle, \dots, |\phi_L\rangle\} \\ \{|\phi_1\rangle, |\phi_2\rangle, \dots, |\phi_{a-1}\rangle, |\phi_a^{m+}\rangle, |\phi_{a+1}\rangle, \dots, |\phi_L\rangle\} \\ \{|\phi_1\rangle, |\phi_2\rangle, \dots, |\phi_{a-1}\rangle, |\phi_a^{m-}\rangle, |\phi_{a+1}\rangle, \dots, |\phi_L\rangle\} \end{cases}$$

and employing one of these three basis states set which gives the lowest energy. The chosen basis state  $|\phi_a^{m-1}\rangle$ ,  $|\phi_a^{m+}\rangle$  or  $|\phi_a^{m-}\rangle$  is taken to be a next basis state  $|\phi_a^m\rangle$ .

$\rightarrow$  *computation time*  $\propto L^3$

- Repeat the above local interaction projection for all the sites  $m = 1, 2, \dots, N$ .
- Repeat the above  $\exp[-\Delta\tau\hat{H}]|\phi_a\rangle$  projection for all basis states  $a = 1, 2, \dots, L$ .

$$\implies \text{The total computation time} \propto L^2N^3 + L^4N \quad (3.9)$$

Though the basic computation time of PIRG is listed above, an efficient convergence procedure is important for reducing the computation time. There may appear many states with local minima structure in energies in the PIRG convergence process. Even if the convergence is not perfect, which is actually the case in most of our experience, the extrapolation procedure can be performed for the ground state properties. However, the worse converged state gives the value with larger error. Because the extrapolation itself using the energy variance is the formalism to obtain values of an eigenstate of the Hamiltonian, in case of worse convergence than a limit, the extrapolation procedure could give the value not for the ground state but for an excited state. Therefore it is important to improve PIRG convergence process by a combination with some existing methods to avoid occurrence of trapping in local minima. At present, we have empirically learned that the sufficient convergence at small subspace is crucial at the early stage of the process of extending  $L$ . In this paper, we have numerically realized convergence to the state of the Hartree-Fock approximation at  $L = 1$  and iterated hundreds projections at small  $L$ , for example for  $L$  less than 10. However more systematic methods are desired and are left for future studies.

### 3.2.2 Details on reduction of computation time

Since inner products and Hamiltonian elements are calculated from determinants and inverse matrices, the computation time for them is usually proportional to  $N^3$ . In the process of local-interaction projection, however, it can be reduced to  $N^2$ .

Here, to explain the procedure to reduce the computation time from  $N^3$  to  $N^2$ , we simply consider the state  $\sum_{k=1}^N [M_1(s)]_{ik} [\phi_{a\sigma}]_{kj}$  in Eq.(3.7) for the following discussion. When the basis state of the  $a$ -th Slater determinant with spin  $\sigma$  is updated by the projection of the  $m$ -th site local interaction as,

$$[\phi_{a\sigma}]_{kj} \Rightarrow \sum_{k=1}^N [M_1(s)]_{ik} [\phi_{a\sigma}]_{kj} \quad (3.10)$$

the inner products change as,

$$\langle \phi_{a\sigma} | \phi_{b\sigma} \rangle \Rightarrow \begin{cases} \left(1 + \delta(s) \left[ G_{\sigma}^{ab} \right]_{mm} \right) \times \langle \phi_{a\sigma} | \phi_{b\sigma} \rangle & \text{for } b \neq a \\ \left(1 + \delta(s) \left[ \tilde{G}_{\sigma}^{ab} \right]_{mm} \right) \times \langle \phi_{a\sigma} | \phi_{b\sigma} \rangle & \text{for } b = a \end{cases} \quad (3.11)$$

and the Green's functions change as,

$$\left[ G_{\sigma}^{ab} \right]_{ij} \Rightarrow \begin{cases} \left( \delta(s) \delta_{im} + 1 \right) \left( \left[ G_{\sigma}^{ab} \right]_{ij} - \frac{\left[ G_{\sigma}^{ab} \right]_{im} \delta(s) \left[ G_{\sigma}^{ab} \right]_{mj}}{1 + \left[ G_{\sigma}^{ab} \right]_{mm} \delta(s)} \right) & \text{for } b \neq a \\ \left( \delta(s) \delta_{mj} + 1 \right) \left( \left[ \tilde{G}_{\sigma}^{ab} \right]_{ij} - \frac{\left[ \tilde{G}_{\sigma}^{ab} \right]_{im} \delta(s) \left[ \tilde{G}_{\sigma}^{ab} \right]_{mj}}{1 + \left[ \tilde{G}_{\sigma}^{ab} \right]_{mm} \delta(s)} \right) & \text{for } b = a \end{cases} \quad (3.12)$$

where

$$\left[ \tilde{G}_{\sigma}^{ab} \right]_{ij} = \left( \delta(s) \delta_{im} + 1 \right) \left( \left[ G_{\sigma}^{ab} \right]_{ij} - \frac{\left[ G_{\sigma}^{ab} \right]_{im} \delta(s) \left[ G_{\sigma}^{ab} \right]_{mj}}{1 + \left[ G_{\sigma}^{ab} \right]_{mm} \delta(s)} \right) \quad (3.13)$$

$$\delta(s) = \exp \left[ 2as - \frac{\Delta\tau U}{2} \right] - 1. \quad (3.14)$$

Here  $i, j$  is from 1 to  $N$  and  $\delta_{im}$  is the Kronecker's  $\delta$  symbol. In this way the computation time for local interaction projection is reduced to that proportional to  $N^2$ . The similar reduction in the computation time is explained in detail in the literature.<sup>1)</sup>

### 3.2.3 Devices on extrapolation procedure

For the extrapolation process after the PIRG convergence, it is necessary to calculate  $\langle \hat{H} \rangle$ ,  $\langle \hat{H}^2 \rangle$ ,  $\langle \hat{H}^3 \rangle$  and expectation values of other operators. Because the Hamiltonian does not have any long-range interaction term, the computation time for  $\langle \hat{H}^n \rangle$  is proportional to  $N^n$  except for the computation time for single particle Green's function  $N^3$ . The coefficient of  $N^n$  is, however, large and it is useful to decrease this computation time by the following procedure.

Because a converged state by PIRG is a linear combination of Slater determinants and the kinetic term projection  $\exp[-\Delta\tau \hat{H}_k]$  does not increase the number of Slater determinants, it is easier to

calculate the right hand side of the following equation than to calculate the left hand side from single particle Green's functions in the following equation:

$$\frac{\langle \psi | \hat{A} \hat{H}_k | \psi \rangle}{\langle \psi | \psi \rangle} = \frac{1}{\Delta\tau} \left( \frac{\langle \psi | \hat{A} | \psi \rangle}{\langle \psi | \psi \rangle} - \frac{\langle \psi | \hat{A} \exp[-\Delta\tau \hat{H}_k] | \psi \rangle}{\langle \psi | \psi \rangle} \right) + O(\Delta\tau), \quad (3.15)$$

where we take sufficiently small  $\Delta\tau$ . In this way, the computation time of the term, such as  $\hat{H}_k^3$ , can be reduced.

### 3.3 Required memory

The largest share of the memory is exhausted for the storage of the elements in all the elements of the Slater determinants in the basis states and also for that of the Green's function. Here we assume scalar information takes *8byte* and the number of basis states  $L$  is 500 to roughly estimate the required maximum memory size. Slater determinant is an  $N \times M$  matrix for each spin, and then near half filling of the Hubbard model, this is comparable to  $N^2$  scalar elements. As we see in (3.3), Green's function is represented by an  $N \times N$  matrix for each spin, and then this contains  $2N^2$  scalars. If we store all the Green's function data among the  $L$  Slater determinants, about *83Gbyte* is necessary for  $12 \times 12$  system and it cannot be easily stored in our available computer. For this reason, we store only the Green's function between the Slater determinant just on the operation of  $\exp[-\Delta\tau \hat{H}]$  and the others. Then the necessary memory for the state and Green's function is the order of  $3LN^2 \times 8\text{byte}$ , which is about *250Mbyte* for  $12 \times 12$  system.

### 3.4 Parallelization

Parallelization of a code is a promising way to improve the performance of the computation by dividing a large set of calculations into several smaller pieces and execute them independently of each other. We have tried to parallelize the code on the distributed memory system using MPI. As shown in Eq.(3.9), the computation time for a single slice projection  $\exp[-\Delta\tau \hat{H}]$  is proportional to  $L \times (LN^3 + L^3N)$ . Because the first factor  $L$  refers to the iteration on all the basis states which are related to each other in the evaluation of the energy, it is difficult to parallelize this process. Then we consider the parallelization of the part  $LN^3 + L^3N$ .

The first term  $LN^3$  is related to the calculation of inner products and Green's functions between a basis state on the operation and the other basis states. Each calculation is independent and it can be parallelized. For this parallelization, the memory for each state and each Green's function have to be distributed over each processor. For example, the 1-st state and the 1-st Green's function are on the 1-st processor memory, and the 2-nd state and the 2-nd Green's function are on the 2-nd processor memory, etc..

The second term  $L^3N$  is related to the iteration of the calculation of the lowest energy of the stored Hilbert subspace by Eq.(2.16) for each local projection. The matrix related to this generalized

eigenvalue problem is  $L \times L$ . In practice,  $L$  is the order of hundreds and it is difficult to parallelize efficiently the eigenvalue problem of such a small matrix. However by performing the projection  $\exp[-\Delta\tau\hat{H}]$  for some different choices of  $\Delta\tau$  in parallel and employing the result which gives the lowest energy among the choices of  $\Delta\tau$ , the convergence becomes faster and computation time for Eq.(2.16) does not increase. In this way, we can reduce the total computation time for convergence by parallelization.

## §4. Evaluation of PIRG on Hubbard model

### 4.1 Model

We apply PIRG to the Hubbard model Hamiltonian (2.3) on a two-dimensional square lattice with nearest-neighbor transfers  $t$ .

$$t_{ij} = \begin{cases} t = 1.0 & \text{if } (i, j) \text{ are the nearest neighbor sites} \\ 0 & \text{otherwise} \end{cases} \quad (4.1)$$

We take  $t = 1.0$  as the energy scale. Since these models have particle-hole symmetry at half filling, the quantum Monte Carlo does not suffer from the sign problem at half filling. By comparing with the QMC and exact diagonalization results in the literature, we show PIRG results on the energy, the momentum distribution and the equal-time spin correlations and discuss the accuracy and efficiency of PIRG on these models.

### 4.2 Comparison of energy

#### 4.2.1 PIRG result

First, we show the converged results by PIRG before the extrapolation procedure and discuss the relative error. In §2 we refer to the DMRG method in which the relative error decreases exponentially as a function of the dimension of the stored Hilbert subspace. Because there is a restriction on the choice of basis in PIRG, the relative error dependence on the dimension of the stored Hilbert subspace is different between DMRG and PIRG. Figure 2 shows the relative error and Figs. 3 and 4 show the relative difference between PIRG and QMC results. In case of a small system such as  $6 \times 2$  Hubbard model, the relative error is smaller than 1 percent. For larger systems near half filling, the relative error is larger but less than a few percent independent of the system size. This feature holds both at half filling and near half filling. Note that the results at  $L = 1$  correspond to the Hartree-Fock estimates.

#### 4.2.2 Extrapolation results

The above results are improved to more accurate estimates by the extrapolation procedure. Here we show the simple extrapolation results  $E$  with the state  $|\phi\rangle$  and the extrapolation results  $E_{sqr}$  with the state  $\sqrt{\hat{H}}|\phi\rangle$  for the same  $6 \times 6$  Hubbard model by taking  $L$  up to 256. Both extrapolation

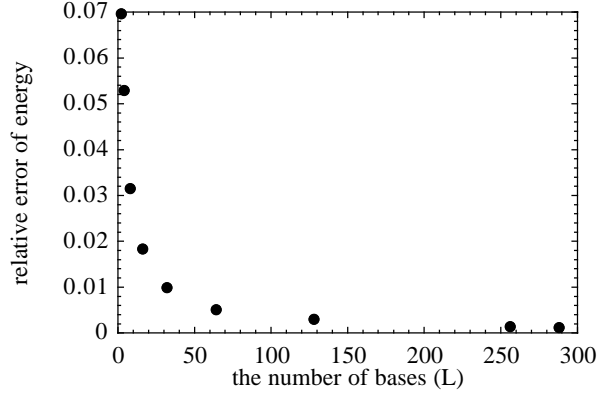


Fig. 2. Relative error  $\delta E/|E|$  in the ground state energy for the  $6 \times 2$  Hubbard model with 5 up 5 down electrons and the fully periodic boundary condition at  $U/t = 4.0$ . The reference ground state energy is estimated from the exact diagonalization.

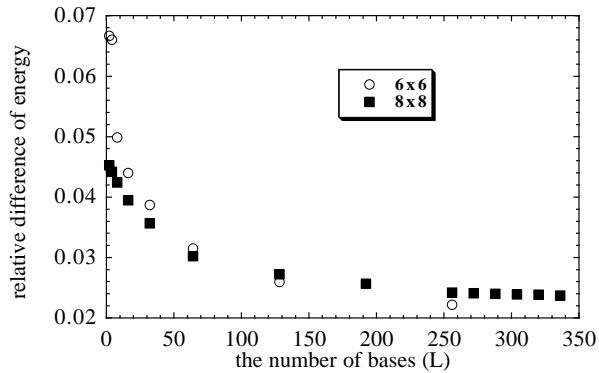


Fig. 3. Relative difference  $\delta E/|E|$  in the ground state energy for the Hubbard models at half filling with the fully periodic boundary condition at  $U/t = 4.0$ . The reference ground state energy is estimated from QMC.<sup>2)</sup>

procedures for two models are shown in Figs. 5 and 6. Two extrapolated results should meet at the same value in principle, although there is a small difference, which may be thought to be PIRG error. Because we do not know which one is closer to the exact value and empirically it is better for the linear function fitting to use the value obtained from the state  $\sqrt{\hat{H}}|\phi\rangle$ , hereafter we employ the extrapolation using  $\sqrt{\hat{H}}|\phi\rangle$ . The relative errors and differences after the extrapolation are shown in Table I. For most of the systems, PIRG can give results of the ground state energy with less than 0.3 percent relative error or difference from QMC results.

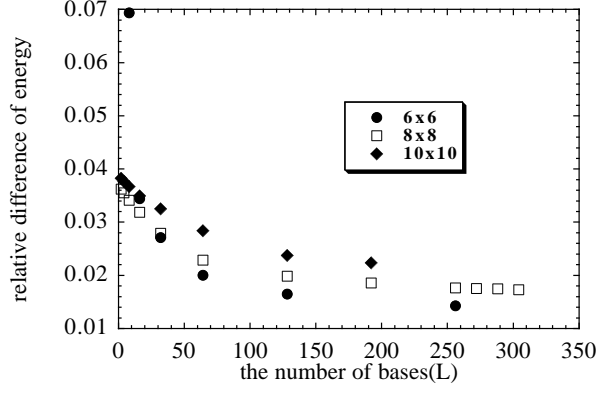


Fig. 4. Relative difference  $\delta E/|E|$  in the ground state energy for the Hubbard models with two hole doped from half filling and fully periodic boundary condition at  $U/t = 4.0$ . The reference ground state energy is estimated from QMC.<sup>2)</sup>

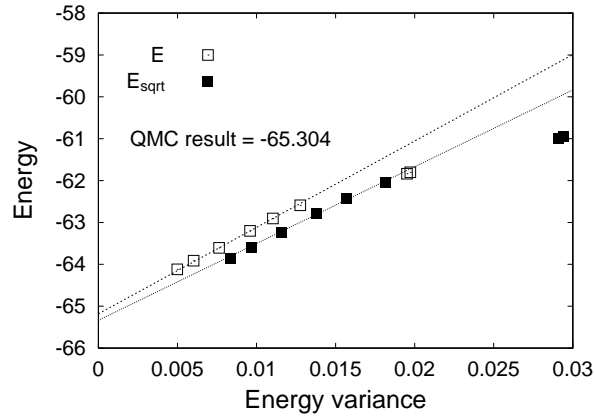


Fig. 5. Extrapolation of the energy to the zero energy variance for a  $6 \times 6$  Hubbard model, 17 up 17 down electrons with the fully periodic boundary condition at  $U/t = 4.0$

### 4.3 Comparison for other physical quantities

Next, we evaluate the equal-time spin correlations and the momentum distribution on  $6 \times 2$  Hubbard model, 5 up 5 down electrons with the fully periodic boundary condition at  $U/t = 4.0$ . In our study, the equal-time spin correlations in the momentum space is calculated from,

$$S(\mathbf{q}) = \frac{1}{3N} \sum_{i,j}^N \langle S_i S_j \rangle e^{i\mathbf{q}(\mathbf{R}_i - \mathbf{R}_j)} \quad (4.2)$$

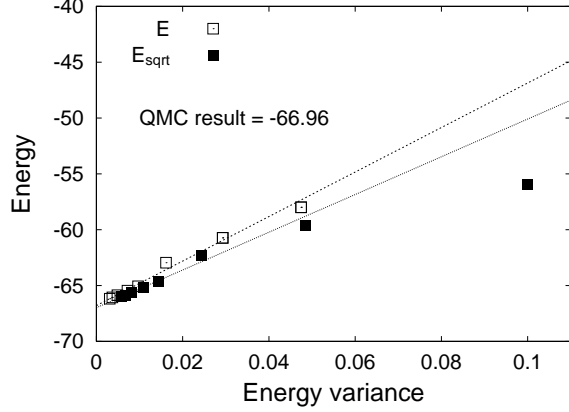


Fig. 6. Extrapolation of the energy to the zero energy variance for a  $6 \times 6$  Hubbard model, 18 up 18 down electrons with the fully periodic boundary condition at  $U/t = 4.0$

Table I. relative error and difference of the ground state energy after extrapolation.

system	PIRG results	exact diagonalization and Monte Carlo results	relative difference or error
$6 \times 2, 5 \uparrow, 5 \downarrow$	$-25.6999 \pm 0.0005$	$-25.6952$	0.00018
$6 \times 6, 17 \uparrow, 17 \downarrow$	$-65.12 \pm 0.02$	$-65.30 \pm 0.04$	0.0028
$6 \times 6, 18 \uparrow, 18 \downarrow$	$-66.92 \pm 0.04$	$-66.96 \pm 0.07$	0.00060
$8 \times 8, 31 \uparrow, 31 \downarrow$	$-117.8 \pm 0.1$	$-117.70 \pm 0.06$	0.00085
$8 \times 8, 32 \uparrow, 32 \downarrow$	$-119.4 \pm 0.1$	$-119.23 \pm 0.06$	0.0014

where  $S_i$  is the spin of the  $i$ -th site and each element of the spin is calculated from

$$\begin{aligned}
 S_i^x &= \frac{1}{2} (S_i^+ + S_i^-) = \frac{1}{2} (c_{i\uparrow}^\dagger c_{i\downarrow} + c_{i\downarrow}^\dagger c_{i\uparrow}) \\
 S_i^y &= \frac{1}{2i} (S_i^+ - S_i^-) = \frac{1}{2i} (c_{i\uparrow}^\dagger c_{i\downarrow} - c_{i\downarrow}^\dagger c_{i\uparrow}) \\
 S_i^z &= \frac{1}{2} (n_{i\uparrow} - n_{i\downarrow}).
 \end{aligned} \tag{4.3}$$

All the extrapolation behaviors of the equal-time spin correlations are shown in Figs.7 and 8. The results after the extrapolation procedure are shown in Table II. Here we take the lattice constant to be unity.

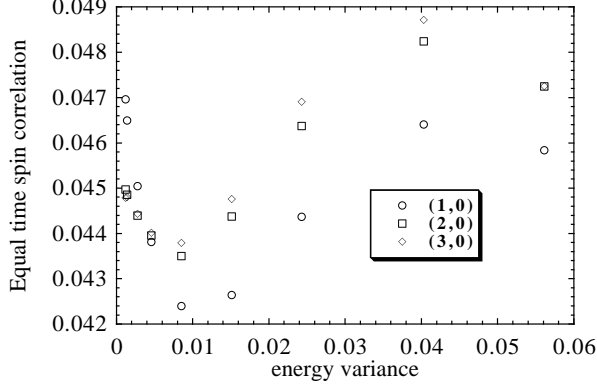


Fig. 7. The extrapolation of the equal-time spin correlations  $S(k_x, k_y)$  to zero energy variance for the  $6 \times 2$  Hubbard model with 5 up 5 down electrons with the fully periodic boundary condition at  $U/t = 4.0$ . The wavenumber  $(k_x, k_y)$  for each symbol is given in the inset.

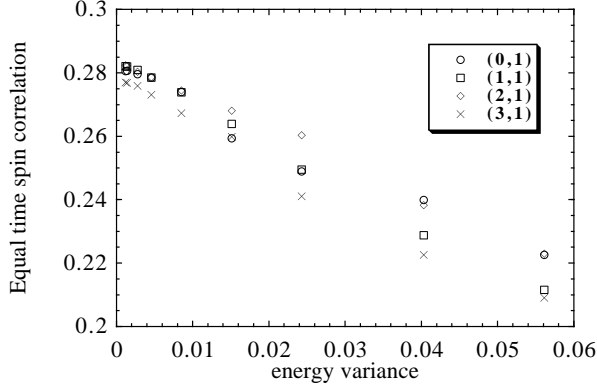


Fig. 8. The extrapolation of the equal-time spin correlations  $S(k_x, k_y)$  to zero energy variance for the  $6 \times 2$  Hubbard model with 5 up 5 down electrons with the fully periodic boundary condition at  $U/t = 4.0$ . The wavenumber  $(k_x, k_y)$  for each symbol is given in the inset.

The momentum distribution is calculated from,

$$n(\mathbf{q}) = \frac{1}{2N} \sum_{i,j}^N \langle c_{j\uparrow}^\dagger c_{i\uparrow} + c_{j\downarrow}^\dagger c_{i\downarrow} \rangle e^{i\mathbf{q}(\mathbf{R}_i - \mathbf{R}_j)} \quad (4.4)$$

where  $\mathbf{R}_i$  is the vector representing the place of the  $i$ -th site. All the extrapolation behaviors of the momentum distribution are shown in Figs.9 and 10. The comparison of the results after the extrapolation is shown in Table III.

Among the equal-time spin correlations and the momentum distribution, some of them have relatively large errors of about a few percents. Most of the relative errors are, however, less than 1

Table II. The equal-time spin correlations  $S(k_x, k_y)$  for the  $6 \times 2$  Hubbard model with 5 up 5 down electrons with the fully periodic boundary condition at  $U/t = 4.0$

$(k_x, k_y)$	PIRG	exact diagonalization	relative error
(1,0)	0.0482	0.0488	0.012
(2,0)	0.0454	0.0458	0.0044
(3,0)	0.0451	0.0457	0.013
(0,1)	0.281	0.277	0.014
(1,1)	0.283	0.281	0.0071
(2,1)	0.284	0.286	0.0070
(3,1)	0.278	0.279	0.0036

percent.

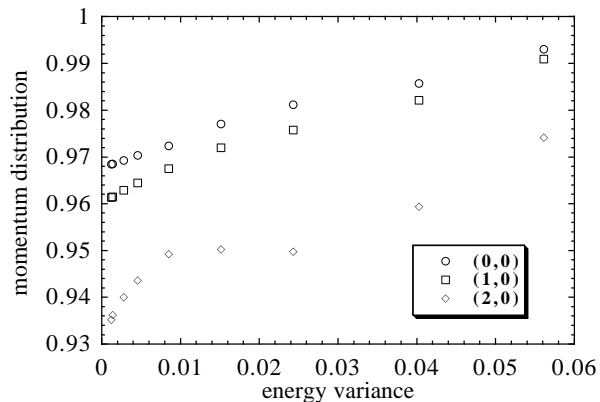


Fig. 9. The extrapolation of the momentum distribution  $n(k_x, k_y)$  to zero energy variance for the  $6 \times 2$  Hubbard model with 5 up 5 down electrons with the fully periodic boundary condition at  $U/t = 4.0$ . The wavenumber  $(k_x, k_y)$  for each symbol is given in the inset.

## §5. Summary

Path-integral renormalization group(PIRG) is a numerical algorithm for studying the ground state properties. The process filtering out the ground state  $|\psi_g\rangle$  is performed in the imaginary time

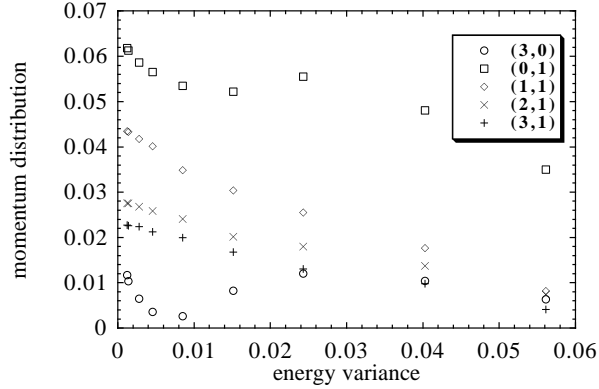


Fig. 10. The extrapolation of the momentum distribution  $n(k_x, k_y)$  to zero energy variance for the  $6 \times 2$  Hubbard model with 5 up 5 down electrons with the fully periodic boundary condition at  $U/t = 4.0$ . The wavenumber  $(k_x, k_y)$  for each symbol is given in the inset.

Table III. The momentum distribution  $n(k_x, k_y)$  for the  $6 \times 2$  Hubbard model with 5 up 5 down electrons with the fully periodic boundary condition at  $U/t = 4.0$

$(k_x, k_y)$	PIRG	exact diagonalization	relative error
(0,0)	0.9678	0.9681	0.00031
(1,0)	0.9604	0.9601	0.00031
(2,0)	0.9288	0.9281	0.00075
(3,0)	0.02067	0.01850	0.092
(0,1)	0.06515	0.06806	0.044
(1,1)	0.04504	0.04513	0.0017
(2,1)	0.02821	0.02787	0.012
(3,1)	0.02294	0.02281	0.0057

direction as,

$$|\psi_g\rangle = \lim_{\tau \rightarrow \infty} \exp[-\tau \hat{H}] |\phi_{initial}\rangle.$$

Therefore its formalism can be applied to any kind of systems and there is no restriction on the spatial dimension of the system. In this path-integral formalism, the ground state is represented by chosen basis states  $|\phi\rangle$ ,

$$|\psi_g\rangle = \sum_i c_i |\phi_i\rangle.$$

By the numerical renormalization, relevant basis states are selected and irrelevant basis states are projected out. This makes it possible to calculate the approximate ground state directly as an optimized linear combination of chosen basis states:

$$|\psi_g\rangle \approx \sum_{i=1}^L w_i |\phi_i\rangle.$$

Therefore there is no negative sign problem even in frustrated systems. In this way, PIRG can be applied to the systems which can not be treated by existing algorithms such as the quantum Monte Carlo method or the density matrix renormalization group.

Because the converged state by PIRG is an approximate ground state under the restriction on the number of the basis states, the exact ground state can be achieved by the extrapolation of the number of states  $L$  to the dimension of the whole Hilbert space. We have shown the general extrapolation procedure in this paper:

$$\langle \hat{H} \rangle - \langle \hat{H} \rangle_g \propto \Delta E$$

where  $\Delta E$  is the energy variance,

$$\Delta E = \frac{\langle \hat{H}^2 \rangle - \langle \hat{H} \rangle^2}{\langle \hat{H} \rangle^2},$$

$\langle \quad \rangle_g$ , the expectation value in the true ground state and  $\langle \quad \rangle$ , the expectation value in an approximate ground state. This relation holds for sufficiently converged approximate state. We confirm that the results of more than a hundred Slater determinants follow the above relation and can be used for a linear extrapolation in the Hubbard model. On the physical quantity  $\hat{A}$ , a similar relation holds in most cases.

$$\langle \hat{A} \rangle - \langle \hat{A} \rangle_g \propto \Delta E.$$

For short-ranged correlation functions, the linearity holds at the same level as the energy in the thermodynamic limit. By these extrapolation procedure, more accurate results are obtained while the variational principle is not strictly satisfied after the extrapolations.

We compare the expectation values of the energy, the momentum distribution and the equal-time spin correlations with those of exact diagonalization on  $6 \times 2$  lattice systems and with those of quantum Monte Carlo on larger systems. For the momentum distribution and the equal-time spin correlations, the relative errors and differences from QMC are less than a few percents. Especially on the energy, the relative errors and differences from QMC have three digits accuracy. We confirm that these accuracy can be achieved up to  $12 \times 12$  systems on the square lattice.

We have also explained the dependence of the computation time as  $L^2 N^3 + L^4 N$  where  $N$  is the system size and  $L$ , the dimension of the stored PIRG Hilbert subspace. We refer to some implementation advice on PIRG and the efficiency of distributed memory parallelization on PIRG methods. Because in general it is difficult to parallelize efficiently the operations of matrices with

the size such as hundreds  $\times$  hundreds or the iteration process, it is necessary to change the algorithm to make the convergence faster by projecting some basis states in parallel.

In this study, we have dealt with Hubbard models using Slater determinants as PIRG basis states. Applications of PIRG to other systems are very interesting and promising future projects.

## Acknowledgments

The authors thank F. F. Assaad for useful comments. This work is supported by the ‘Research for the Future’ program from the Japan Society for the Promotion of Science under grant number JSPS-RFTF97P01103. A part of our computation has been done at the supercomputer center at the Institute for Solid State Physics, University of Tokyo.

## Appendix: Inner product of Slater determinants

Here we ignore the spin degrees of freedom for simplicity. A Slater determinant  $|\phi_a\rangle$  is represented to be an  $N \times M$  matrix  $[\phi_a]$ .

$$|\phi_a\rangle = \prod_{j=1}^M \left( \sum_{i=1}^N [\phi_a]_{ij} c_{i\sigma}^\dagger \right) |0\rangle. \quad (\text{A}\cdot 1)$$

where  $a$  is a symbol to distinguish Slater determinants. Eq.(3.2) can be obtained as the following:

$$\langle \phi_a | \phi_b \rangle = \langle 0 | \prod_{j=1}^M \prod_{l=1}^M \left( \sum_{i=1}^N [\phi_a]_{ij} c_i \right) \left( \sum_{k=1}^N [\phi_b]_{kl} c_k^\dagger \right) |0\rangle \quad (\text{A}\cdot 2)$$

$$= \sum_{\mathbf{S}}^{N C_M} \left\{ \sum_{\mathbf{n}}^{M!} \sum_{\mathbf{m}}^{M!} \text{sgn}(\mathbf{n}) \text{sgn}(\mathbf{m}) \prod_{j=1}^M \left( [\phi_a]_{\mathbf{S}_{\mathbf{n}(j)j}} [\phi_b]_{\mathbf{S}_{\mathbf{m}(j)j}} \right) \right\}. \quad (\text{A}\cdot 3)$$

Here  $\mathbf{n}$  and  $\mathbf{m}$  are permutation of  $M$  symbols:

$$\mathbf{n} = \begin{pmatrix} 1, & 2, \dots, & M \\ \mathbf{n}(1), \mathbf{n}(2), \dots, \mathbf{n}(M) \end{pmatrix}, \quad (\text{A}\cdot 4)$$

the same is assumed for  $\mathbf{m}$ ;  $\sum_{\mathbf{n}}^{M!}$  means taking the sum over all permutations of  $M$  symbols;  $\text{sgn}(\mathbf{n})$  is the signature of the permutation  $\mathbf{n}$ :

$$\text{sgn}(\mathbf{n}) = \begin{cases} +1 & \text{for an even permutation} \\ -1 & \text{for an odd permutation} \end{cases}; \quad (\text{A}\cdot 5)$$

$\mathbf{S}$  is a set of  $M$  numbers chosen from  $N$  numbers  $1, 2, \dots, N$  and we assume the ascendent order on this set  $\mathbf{S}$ ;  $\sum_{\mathbf{S}}^{N C_M}$  means taking the sum over all combinations of  $M$  numbers. Then the inner product can be transformed from Eq.(A-3) as the following:

$$\langle \phi_a | \phi_b \rangle = M! \sum_{\mathbf{S}}^{N C_M} \left\{ \sum_{\mathbf{n}}^{M!} \text{sgn}(\mathbf{n}) \prod_{j=1}^M \left( [\phi_a]_{\mathbf{S}_{j j}} [\phi_b]_{\mathbf{S}_{\mathbf{n}(j)j}} \right) \right\} \quad (\text{A}\cdot 6)$$

$$= M! \sum_{\mathbf{S}}^{N C_M} \left\{ \sum_{\mathbf{n}}^{M!} \text{sgn}(\mathbf{n}) \prod_{j=1}^M \left( [\phi_a]_{\mathbf{S}_{j j}} [\phi_b]_{\mathbf{S}_j \mathbf{n}(j)} \right) \right\} \quad (\text{A}\cdot 7)$$

$$= \sum_{\mathbf{n}} \frac{M!}{\mathbf{n}!} \text{sgn}(\mathbf{n}) \prod_{j=1}^M \left( \sum_{i=1}^N [\phi_a]_{ij} [\phi_b]_{i\mathbf{n}(j)} \right) \quad (\text{A}\cdot 8)$$

$$= \det \left( {}^t [\phi_a] [\phi_b] \right). \quad (\text{A}\cdot 9)$$

- 1) M.Imada and Y.Hatsugai: J.Phys.Soc.Jpn.**58**(1989)3752.
- 2) N.Furukawa and M.Imada: J.Phys.Soc.Jpn.**61**(1992)3331.
- 3) S.R.White: Phys.Rev.**B48**(1993)10345.
- 4) T.Nishino: J.Phys.Soc.Jpn.**64**(1995)3598.
- 5) N.Shibata: J.Phys.Soc.Jpn.**66**(1997)2221.
- 6) N.Shibata: Phys.Rev.**B56**(1997)5061.
- 7) M.Imada and T.Kashima: J.Phys.Soc.Jpn.**69**(2000)2723.
- 8) S.Sorella: preprint, cond-mat/0009149
- 9) P.Prelovšek and X.Zotos: Phys.Rev.**B47**(1993)5984
- 10) J.Riera and E.Dagotto: Phys.Rev.**B48**(1993)9515
- 11) N.A.Modine and E.Kaxiras: Phys.Rev.**B53**(1996)2546
- 12) H.D.Raedt and W.v.d.Linden: Phys.Rev.**B45**(1992)8787
- 13) M.Honma, T.Misusaki and T.Otsuka: Phys.Rev.Lett**75**(1995)1284